Fracture 1977, Volume 1, ICF4, Waterloo, Canada, June 19 - 24, 1977

THE APPLICATION OF RISK ANALYSIS TO THE BRITTLE FRACTURE AND FATIGUE OF STEEL STRUCTURES

A. S. Tetelman* and P. M. Besuner**

ABSTRACT

The key elements of structural risk analysis are described. These elements include the definition, estimation, and assessment of failure mode frequency, severity, and associated risk. Developed risk analysis techniques are used to evaluate a critical steel suspension bridge component and an automobile steering component. The major feature of the developed techniques is the demonstrated improvement in the statistical analysis of structural field performance due to the incorporation of a minimum amount of engineering fracture mechanics analysis.

INTRODUCTION

The aim of optimum structural design is the achievement of reliable performance at minimum cost. Although "cost" and "performance" are defined by standard economic methods, the word "reliable" is ill-defined. It is related to the probability and consequences of a failure, and to the acceptance of those consequences by people who interface with the system. For example, the brittle fracture of a drinking glass that is dropped on the floor is an undesirable but hardly catastrophic event. Although it occurs relatively often, its consequences are generally minor and rarely lead to major injuries or fatalities. On the other hand, the collapse of a large structure, such as a highway bridge, has enormous consequences in terms of both human and economic loss.

The concepts of risk analysis can be used to define if the degree of risk is acceptable to society, and hence the acceptable reliability of large structures. The risk or hazard associated with the use of a given component or product is related to both the frequency, f, and the severity, S, of the failure events that result from its use or exposure. A failure event that leads to a negligibly small amount of property damage and no personal injury (severity of zero) is called an "incident" (e.g., the fracture of a water glass). A failure event which has direct consequences (severity > zero) is called an accident. With respect to accidents resulting from brittle fracture, the frequency factor is the probability, p, that a given component will fail by rapid crack propagation (perhaps after fatigue has caused a critical size crack to develop). The severity, S, can be measured in terms of the dollar cost of the accident that results from the fracture, the number of lost working days (outage time), or the extent of personal injury.

*Professor of Engineering, Materials Department, University of California, Los Angeles, California, U.S.A. 90024, and President, Failure Analysis Associates, Palo Alto, California, U.S.A. 94304.
**Senior Analytical Engineer, Failure Analysis Associates, Palo Alto, California, U.S.A. 94304.

Risk may be quantified in terms of a hazard index, I, by simply multiplying the failure probability, f, by the mean severity, $\bar{S}$, for the particular component

$$I = f \times \bar{S} . \qquad (1)$$

On this basis, the risk due to a large number of low-severity failures can be equivalent to the risk due to one failure that has greater consequences.

The degree of risk acceptance and reasonableness of risk are more complex issues that cannot be defined precisely. In the long run, the reasonableness of a particular risk, either "actual" or "perceived" by society, is related to the general level of risk that those exposed to the risk have already found acceptable or unavoidable (e.g., the risk of fatalities due to old age, disease). This point has been discussed in great detail in recent years [1,2].

Engineering analysis can play a strong role in the estimation of both the probability of failure due to various events, and the severity spectra or the consequence of the event. Figure 1 shows a typical way of plotting the frequency and severity of the failure events. The particular data shown in the plot pertain to automobile accidents. The severity scale has been obtained from a combination of National Safety Council classification (fatalities, major injuries, etc.) and the U.S. Consumer Product Safety Classification (CPSC severity units ranging from 0 to 25,000). Several things are apparent from the figure. First, high severity events occur with less frequency than the low severity events. The inverse relationship between frequency and severity is observed in many natural phenomena such as earthquakes, wind gusts, and floods. Second, the distribution of severity in a given automobile accident is the same whether the accident was caused by a defective vehicle defect or by driver error. This implies that the severity of the initiating event does not depend on whether the event is caused by driver error or an unspecified mechanical defect.

Figure 2 shows a schematic representation of the frequency/severity curve, which has been divided arbitrarily into four partitions. The upper right hand corner (Region 1) represents high frequency, high severity events, where the hazard ($f \times \bar{S} = I$) is high and improvements must be made to reduce either f, $\bar{S}$, or both parameters. The lower left hand corner (Region 3) describes low frequency, low severity events and consequently, at least in a comparative sense, describes low risk events that are of little interest.

In the other two areas (Regions 4 and 2) accurate risk assessment is required to define the need and type of action required. The first area deals with the continued use or the improvement of a product or component that has a relatively high failure rate (based on a record of significant past experience), but for which the mean severity $\bar{S}$ is small (Region 4). If event tree analysis is able to postulate that severe accidents are possible, then it must be shown whether continued usage could lead to (1) an increased $\bar{S}$, (2) an increased f due to time-dependent degradation (i.e., fatigue) and (3) whether the combination of f and $\bar{S}$ is sufficiently large to warrant safety and cost-effective product improvement.

The second area (Region 2) deals with high severity, but low frequency events. There may have been a single, unexpected event of high severity (e.g., a bridge collapse) after a limited amount of service and it is necessary to determine the risk associated with the continued operation

of similar structures. Particularly, it is necessary to determine whether safe operation of similar structures can be achieved by lowering the operating stress level by a given amount, say 20%, or by increasing the frequency of nondestructive inspections (NAT) by a factor of, say two, or by doing both of these things. Alternatively, there may be concern over a real or perceived high severity event where no failures have occurred over a limited amount of service (e.g., catastrophic failure of a nuclear pressure vessel). In these instances, f is so ill-defined* that past failure (and success) experience is not sufficient to make reliable predictions of risk. Risk assessments must then be based on the operational history of similar structures (e.g., non-nuclear pressure vessels), and account must be taken of the differences in stress level, material properties, and maintenance between the nuclear and non-nuclear vessels.

During the past three years, Failure Analysis Associates has developed a variety of techniques to quantify risk associated with mechanical and structural failures. The techniques are based on 1) the statistical analysis of applicable field failure data to determine base line component reliability, and 2) minimum application of conservative engineering models to significantly expand the data base to consider key parameter changes and in those cases where the available data base is too low to allow a high confidence in the reliability estimate. The combination of field data with engineering modelling is called *Combined Analysis* (CA). In those cases where brittle fracture is the dominant failure mode, the analytical tool of most importance is *Probabilistic Fracture Mechanics* (PFM). This tool allows the extension of conventional deterministic *Linear Elastic Fracture Mechanics* (LEFM) to account for variability of K_{Ic}, da/dN, etc. *Combined Analyses* (CA) have been used to make risk assessments for high frequency, low severity type failures, such as fatigue or wear-out failures of automotive components, where failure of a system is generally controllable and does not produce large consequences compared to major disasters such as bridge collapse. Risk assessments by CA have also been made for large structures (bridges, supertankers, HF transmission towers) that have components under tensile stress at temperatures in the vicinity of NDT. In these cases, it is necessary to determine the probability of brittle fracture of key structural members, particularly if there is no redundancy, since fracture of a key member can lead to complete structural collapse of very high severity. It is this latter subject that forms the basis for this plenary lecture.

THE RISK OF BRIDGE COLLAPSE DUE TO BRITTLE FRACTURE

To illustrate the use of the combined analysis (CA) approach to structural reliability, we shall draw on the results of a recent risk assessment that Failure Analysis Associates performed. In 1967, the Point Pleasant Bridge collapsed over the Ohio River, leading to the death of 46 people and a very large economic loss. The collapse resulted from failure of a critical structural member (an eyebar) due to fatigue and/or corrosion, followed by brittle fracture. The bridge was constructed from 1060 steel and experienced relatively high live tensile stresses ($\Delta\sigma$ = 264 MPa at the eyebar surface) at temperatures below NDT ($T_{NDT} \approx 40^0$C). Failure Analysis

*If the failure rate is constant, the best estimate of f is zero and the (95%) upper confidence bound interval estimate is $f_{.95}=3.0/T$ where T is the total (small) exposure time, and the factor 3.0 is based on the 0.95 fractile of the chi-squared probability distribution with two degrees of freedom.

Associates was asked to determine, based on 1) the failure of this one bridge (one data point), 2) the lack of failures in other eyebar bridges, and 3) some laboratory test data, the failure probability of a similar eyebar bridge that was built from a different steel (1035 steel) and subjected to lower nominal stresses, and live stresses ($\Delta\sigma$ = 141 MPa at eyebar surface) at temperatures below NDT($T_{NDT} \approx 20^0$C). We refer below to this subject bridge as the moderately stressed or MS bridge.

All steel bridges, be they girder or suspension bridges, contain structural members that are loaded in tension. Suspension and through-cantilever bridges are literally suspended from steel cables or, alternatively, eyebar links, which are made from sets of eyebars (so called because of their shape). The eyebars are bolted together in sets of two or more. In cases when only two eyebars are used to make up a link, the loads are such that if one eyebar should fail, the second one cannot carry the entire load which is suddenly applied to it. The loading is therefore "non-redundant", such that eyebar failure causes link failure. If the link comprising the two eyebars is, in turn, also non-redundant with respect to the bridge, eyebar failure leads to bridge collapse. This happened in the case of the Point Pleasant Bridge failure. However, in most bridge structures, many (up to 12) of these eyebars are bolted into a link; and if one, two, or even three eyebars fail, the link will not fail. Eyebar failure, then, does not always lead to link failure and bridge collapse.

The bridge that we analyzed contained some two-eyebar, non-redundant links such that an eyebar failure could possibly lead to bridge collapse. It was therefore necessary to determine the probability of eyebar failure to assess the structural reliability of the bridge. As in most structural reliability problems of this type, it was first necessary to locate and search for existing failure data bases, to obtain failure rate data for comparative purposes. Engineering stress and fracture mechanics analyses were then applied to the failure rate data, to account for differences in stress level, materials properties, and other significant parameters between those of the subject bridge and those included in the data base. Table 1 summarizes the data collected on bridges with various characteristics. The first row is for all bridges in the inventory. These exhibit a very low failure rate per bridge-year (about 10^{-6} fpby). Nine of the ten failures (collapses) occurred in welded and steel girder bridges, rather than in through-cantilever, eyebar bridges.

Bridges of the through-cantilever, suspension variety, which was the same type of bridge as both the subject bridge and the Point Pleasant Bridge, were also considered separately. Since only 64 of these steel suspension bridges had been constructed, and since one of them (Point Pleasant) had failed, the point estimate of failure rate for all steel suspension bridges was relatively high. Three* of the sixty-four bridges had 1060 steel eyebars subjected to relatively high stress levels. The failure rate of these, per bridge-year, is very high (8×10^{-3} fpby). Of the other 61 suspension bridges in the United States, 14 are made of 1035 steel and have eyebars operating at moderate stress levels or lower. It was possible to obtain accurate documentation as to the number of eyebar failures in these 14 bridges, which are similar in stress level to the subject bridge. We determined that no eyebar had failed (therefore, the

*The Point Pleasant Bridge, and two other bridges, one of which was a twin of the Point Pleasant Bridge (the St. Mary Bridge) and had been closed down; and the other which is a highly redundant structure which is still operating.

best failure rate point estimate is zero) in 17,600 eyebars subjected to moderate stress levels over 40 year periods. This computed failure rate is not sufficient for a risk calculation, because relatively little field data exist so that the upper bound, 95% confidence level estimate would be unacceptably high (5×10^{-3}fpby). Consequently, it is necessary to modify the point and confidence interval estimates with engineering inputs, and hence we have performed the Combined Analysis (CA) described below.

Following the survey of bridge and eyebar failures, and the failure analysis of the Point Pleasant Bridge, the critical failure mode of the moderately stressed, non-welded bridge was identified as fatigue failure of an eyebar, which could possibly lead to bridge collapse. The bridge reliability problem was then focused on the reliability of eyebars subjected to moderate stress levels (MS). The MS eyebars are constructed from materials that have lower carbon content and lower tensile strength levels (590 MPa vs. 810 MPa) than those used in the Point Pleasant bridge. Consequently, these steels are less susceptible to environmentally-induced, stress corrosion cracking, which was identified as a possible initiation mode of fracture initiation (besides fatigue), in the Point Pleasant failure. Since the rate of fatigue crack growth varies approximately as the fourth power of the live stress level (actually, n = 4.34, inferred from fatigue data), and since the MS bridge is less sensitive to the corrosive effects of the environment than the Point Pleasant Bridge, the rate of crack growth in the MS eyebars is expected to be at least $(264/141)^{4.34} = 15$ times slower than in the Point Pleasant eyebars. If we assume that the same size initial defects, a_i, are present in both the moderately stressed and highly stressed eyebars, then the *mean life* of the MS eyebar is at least 15 times greater than that of the highly stressed eyebar.

Field data were used to determine the frequency of failure for a highly stressed eyebar. There was the one failure (Point Pleasant) in 664 similarly loaded and stressed eyebars on three bridges, each with about 40 years of service. This gives an average eyebar failure rate of 4×10^{-5} failures per eyebar-year and an eyebar failure probability of 1.5×10^{-3} for the first 40 years. Two approaches can be utilized to predict the failure probability of the MS eyebars (and hence the MS bridge). In the simple analysis, the fatigue properties of actual Point Pleasant material, which had been evaluated by a conventional (S/N) curve (Figure 3), were used to obtain the *scatter* in eyebar fatigue life. The scatter in test data is a key parameter in a combined analysis, since it also defines the scatter in service data for nominally identical eyebars subjected to the same stress spectra, and hence defines the failure probability of both the Point Pleasant Bridge and the subject, MS bridge. There is significant scatter in the fatigue data due to natural material variation and the variation in surface condition (i.e., initial size of corrosion pits) following 40 years of service. There is also a logarithmic relationship between stress and mean fatigue life with an exponent of 4.34, which is typical of this kind of failure mode. If the log-normal time-to-failure model is used, the first failure in 664 eyebars corresponds to a failure 2.97 standard deviations from the mean regression line, as shown in Figure 3. This data point also defines a certain number of "reference" laboratory test cycles corresponding to 40 years of bridge life. In other words, assuming that laboratory corrosion fatigue tests accurately represent field conditions, then the scatter in field and laboratory data will be identical. Consequently, the one field failure in 664 similarly stressed eyebars indices to a first laboratory failure at about 13,000 cycles, if 664 test samples had been run.

A vertical line was then drawn to point M, which accounts for the 46% reduction of cyclic stress between the Point Pleasant Bridge and the subject MS bridge. Point M lies almost nine standard deviations from the mean regression line for fatigue failure in this steel, both in the laboratory and hence in the field. Using any reasonable time-to-failure distribution function (log-normal, Weibull) to model fatigue, this indicates a negligible to very low failure probability for the MS eyebars (for log-normal about 10^{-17} in the first 40 years of service). If we assume that the MS bridge contains 1,000 eyebars, 64 of which are non-redundant and hence critical, then the failure probability (calculated with the log-normal model) of the MS bridge over the first 40 years of service is about 6×10^{-16}, which is also negligible. Basically, this simple analysis indicates that a factor-of-two reduction in stress level (along with no change in material fatigue strength level) results in a 2×10^{12} decrease in failure probability. It is significant to note that although the mean life was increased by a factor of 15, the calculated failure probability was decreased by a factor of 2×10^{12}. This is because of the nature of the log-normal distribution of fatigue lives, such that the failure probability decreases dramatically as the tail of the distribution is reached.

A more refined reliability analysis was then performed based on the methods of linear elastic fracture mechanics. The rate of fatigue crack growth is given by the relation

$$da/dN = D(\Delta K)^n = D(\sigma\sqrt{\pi a})^n \ , \qquad (2)$$

where D is primarily a function of the environment in which the material functions. The fracture toughness K_{IC} and the peak tensile stress have little affect on the fatigue life of a brittle steel part, since most of the lifetime of the part is experienced when the crack is small. If two components have the same initial crack size a_i, (e.g., a large corrosion pit, 1 mm deep) then the ratio (C) of fatigue lives of two components operated at stress levels σ_1 and σ_2 in environments characterized by (D_1) and (D_2), is

$$C = \left(\frac{N_1}{N_2}\right) = \frac{D_2}{D_1}\left(\frac{\sigma_2}{\sigma_1}\right)^n \ . \qquad (3)$$

Consequently, if extensive field data are available to determine the lifetime N_1 under a set of conditions denoted as (1), then the mean life under condition set (2) can be determined from a knowledge of C and N_1. Thus

$$N_2 = \frac{N_1}{C} \ . \qquad (4)$$

N_2 thus defines the mean or characteristic lifetime of the subject structure.

The failure probability and usage lifetime, t, often follow a two-parameter untruncated Weibull distribution function

$$F(t) = 1 - \exp(-(t/\beta)^{\alpha}) \qquad (5)$$

where β = distribution scale parameter, which reflects *characteristic* lifetime; mathematically, the lifetime at which F = 0.63.

α = distribution shape parameter which reflects the *scatter* of lifetimes.

The Weibull distribution with its fat lower tail is by far the most conservative of the usually applied time-to-failure models to use for early life failure probability estimates.

As described in detail in [2], laboratory test data are most often used to predict the life scatter parameter α, since at least ten failure data points are required for reasonably accurate estimation of α. The standard deviation of log N about the data mean regression line for eyebar fatigue failure was calculated from 50 data points in Figure 3 to be S = 0.2159. The Weibull scatter parameter α is related to S by [3]

$$\alpha = \frac{.557}{S} \qquad (6)$$

so that

$$\alpha = 2.60 \qquad (7)$$

is the best available characterization of fatigue life scatter from eyebar material with as-received surfaces.

Field failure data are usually required to estimate the characteristic life β under a set of known conditions, or under different conditions if the parameter C in Equation (3) has been determined from fracture mechanics models. Reference [2] indicates that the best estimate for characteristic lifetime of steel eyebars may be obtained from 1) the number of failures (r = 1), 2) the stress levels (σ_i), 3) usage times, (t_i) and 4) corrosion resistances (D_i) of the 17,600 actual bridge eyebars that were summarized in the data base. The formula is

$$\beta_o = \left[\frac{1}{r}\sum_{i=1}^{17,600}(t_i(\sigma_i/\sigma_o)^n/D_i)^{\alpha}\right]^{1/\alpha} = 440 \text{ years} \ , \qquad (8)$$

where n = 4.34 from laboratory fatigue crack growth tests. It was assumed in the analysis of the subject bridge that $D_1/D_2 = 2$, that is, any environmental affects would double the rate of fatigue crack growth in the more susceptible Point Pleasant material, as compared to the subject material, because of the greater possibility of hydrogen cracking in the higher tensile strength material.

Figure 4 plots the Weibull distribution with β_o = 440 years and α = 2.6 and shows the Point Pleasant eyebar failure (at t = 40 years of life) at the correct plotting position for the first failure of 664 similar eyebars (F = .0015). Clearly, from Figure 4, the occurrence of the first failure at 40 years is in good agreement with the independently obtained laboratory fatigue data scatter value of α = 2.6 and provide confirmation of the analytical method. Of course, any failure of the 17,600 MS eyebars would dramatically change the results in Figure 4 and with high confidence, invalidate the analytical method.

Reliability analysis can then be used to account for redundancy and to calculate the probability of structural collapse due to eyebar failure, and hence the failure rate of the subject bridge over the next 15 years of service. The calculated best estimate value is 1.9×10^{-6} failures/year

which is very close to the NBI-based value of 0.95×10^{-6} years $^{-1}$ for all bridges, as shown in Table 1. This further substantiates the combined analysis method described above, and indicates that the risk of failure of the subject bridge is about the same as that of any of the 262,000 bridges in the inventory.

In summary, the CA method, as applied above, requires three basic inputs:

1) Field data under one set of conditions, to define a baseline failure probability (characteristic lifetime).

2) A knowledge or assumption of the *ratio* of stress levels, environmental factors, and the initial flaw sizes between the field environment and the subject environment, to define the constant C and hence the characteristic lifetime N_2 and β_o of the subject structure.

3) Sufficient laboratory tests to define the scatter in relevant parameters (i.e., crack growth rate exponent n), the fatigue life scatter parameter, α.

Once these parameters have been established, the combined analysis may be used to make failure predictions for a variety of design conditions, through proper application of equations (2, 4 and 7).

PROBABILITY OF BRITTLE FRACTURE IN STEEL STRUCTURES

The probability that a structure will fail by brittle fracture is related to three separate and independent parameters:

1) pn(a) - the probability that a flaw of size "a" has been introduced in a unit volume by manufacture or service.

2) P(R|a, s) - the probability that the flaw is rejected by an inspection process, that is sized to reject flaws above a size, s.

3) P(F|a) - the probability of failure, given that a flaw of size "a" exists in structure.

The failure probability P_f of the volume element V_u is then given [4] by the equation

$$P_f \cong V_u \int_o^\infty P(F|a) \left\{1-P(R|a, s)\right\} pn(a)\, da \,. \qquad (9)$$

During the past twenty years, several individual methods and combinations of methods have been developed to reduce the probability of brittle fracture. They are summarized as follows:

1) Minimize pn(a), through the use of specially prepared materials, corrosion protection, careful welding, etc.

2) Maximize P(R|a, s), through the use of increasing inspection sensitivity (minimize flaw size that can be detected) and increasing numbers of inspections (to account for human and mechanical error).

3) Minimize P(F|a), by maintaining low stress levels in materials of low fracture toughness at operating temperature.

All of these procedures lead to increased cost, in decreased performance of increased unit price of material, cost of inspection, or weight of material. The total cost of a structure is a function of the cost of manufacture, C_M, the cost of inspection, C_I, the cost of repair, C_R, and the cost of a failure, C_F. The cost of failure, $C_F P_F$, is accounted for in design and engineering practice either implicitly or explicitly. For example, if the potential cost of a failure is large (e.g., catastrophic brittle fracture of a nuclear pressure vessel), P_F is maintained at a very low level, even though this involves large manufacturing and inspection costs. Alternatively, if C_F is lower (brittle fracture of a railroad car), then P_F can be higher, and the cost per pound for manufacture and inspection of the car will be lower than for the nuclear pressure vessel. At any given period of time, the state of the art and actual engineering practice, as determined by codes and standards, essentially define an "acceptable" P_F for a given type of structure. For example, if the public is more safety conscious, then society treats a failure as being more costly. Consequently, C_F increases, P_F decreases, and C_M and/or C_I increase for a given class of structure. The decrease in P_F as C_F increases is consistent with the hazard $I = f \times S$ remaining constant or decreasing, as more of the population is exposed to the component [1].

In the simplest form, three basic practices exist for design of steel structures against brittle fracture. These are shown schematically in Figure 5. The figure contains a plot of K_{Ic} vs. temperature for structural steels (σ_y < 700 MPa) and high performance, high strength steels (σ_y > 1200 MPa). The data are shown as a band to represent variability in material properties. Also shown are three regions of possible combinations of K and temperature T for each of the given design criteria. The size of the overlap of the K and K_{Ic} bands determines the fracture probability.

Highest ratios of performance of weight based on conventional designs against yielding or fatigue initiation, is achieved with non-redundant high yield strength structural elements, operating at high σ/σ_y ratios. For σ_y = 1200 to 1700 MPa, nominal stress levels of 700 MPa are not uncommon. With K_{Ic} = 50 MP•am$^{1/2}$, this gives critical crack sizes a_c of the order of 1.3 to 2.5 mm in the element. To achieve a failure probability less than, say, 10^{-4} to 10^{-6} per component-year of service, pn(a) must be low and P(R|a, s) must be large. Both of these factors contribute to the very high unit cost of these materials, and to the fact that their usage is generally restricted to military applications where cost is of less significance than in commercial applications.

The second area of interest deals with those structural elements where the catastrophic consequences of a failure dictate that the failure probability must be kept extremely low. High consequences are possible if

1) The structure is non-redundant, such that fracture of a structural element immediately leads to complete brittle fracture of the entire structure,

2) Large amounts of energy and/or harmful species are released by the fracture,

3) Large numbers of people are exposed to the energy or species released,

4) The material cost of the replacement or repair is very large,

5) Leak-before-break is not an acceptable design basis because of the release of dangerous elements.

Nuclear pressure vessels and submarine hulls are two classes of structures that fit into the high consequence category.

An extremely low failure probability can be achieved mostly by maintaining low stresses, but also through low pn(a) and high P(R|a, s) parameters. P(F|a) will generally be lower than for the high performance materials because the nominal stress levels will be lower, of the order of 140 to 280 MPa as compared with 700 MPa. The main guarantee of safety comes through operation of the structure at temperatures well above NDT, such that K_{Ic} and dynamic fracture toughness are both high. For example, if K_{Ic} = 280 $MP\cdot am^{1/2}$ and σ = 280 MPa then a_c = 0.3 m. This value is so improbable (low pn(a_c)) and flaws so detectable (high P(R|a_c, s)) that the failure probability is negligible.

The third area of interest deals with low yield strength constructional steels that are operated at or below NDT temperature. As indicated in Section II, structural elements in bridges made of 1035 (and A-7) steel generally operate below NDT temperature. Other steels such as A-36, API-50, 60 and 70 grades, and A-514 often see operating temperatures below NDT without experiencing brittle fracture.

There are several reasons for this phenomenon, most of which are related to the fact that the probability of fracture initiation is low. These reasons are:

1) The peak nominal stress levels are low, of the order of 30-70 MPa. Consequently, for $K_{Ic} > 50$ $MP\cdot am^{1/2}$, a_c = 0.2 m, even at NDT. The probability that a crack of this size being introduced is remote, provided the structural element is not subjected to abusive loads, and the live (alternating) stresses are maintained below the endurance limit. In those cases where an abusive load is applied (e.g., a bulldozer impacts a pipeline), large flaws are developed and are able to propagate over large distances (hundreds of metres or even kilometres).

2) The initial flaw distribution is low. Large initial flaw sizes are possible only for extremely poor fabrication accidents, in welded structures or in hard zones ($R_c > 25$) which are exposed to hydrogen environments. Some brittle failures have occurred in structural elements subject to these conditions, such as a key member of the Bryte Bend Bridge and an eyebar in the Point Pleasant Bridge. In the former case, the fracture originated at a large weld crack (a = 30 mm) that was exposed to a tensile stress of about 200 MPa. In the latter case, the crack nucleus was a corrosion pit, which in turn initiated a stress corrosion crack in a hard zone in 1060 steel. Although the flaw distribution pn(a) is higher in welded regions as compared with base plate or flanged connections, the presence of a weld and operation below NDT temperature only indicates that brittle fracture is possible, *not that it is probable*. Only a small fraction of welds actually contain defects, and a large fraction of the defects are blunt pores rather than sharp cracks. Consequently, pn($a_{critical}$) is much less than 1.0, rather than being 1.0 as assumed in "worst case" fracture mechanics analysis.

3) High residual stresses are present around some welds; however, many welds are stress relieved. Even those welds that are not stress relieved do not necessarily produce high residual stresses that act over a large volume, V_u. The residual stress gradient around a weld may be quite steep (Figure 6). Consequently, while a brittle fracture may initiate at a weld defect, when $K = K_{Ic}$, it will not be able to propagate ($K = K_{ID}$) outside the heat affected zone, unless the nominal stress level is sufficiently high (minimum 80 to 100 MPa for cracks that extend less than 80 mm into a zone of high residual stress near weld). Figure 7 illustrates the "forbidden" zone where $K < K_{ID}$ and crack arrest occurs near the weld, before the crack grows sufficiently large that it can be propagate in the nominal stress field acting on the entire structural element.

Fourteen years ago, Pellini and Puzak [5] prepared a very significant report in which they described the conditions required for brittle fracture in steel structures. Figure 8, taken from that report, summarizes the classes of brittle fractures they categorized after detailed analysis of many failures. The primary conclusions drawn from this report were 1) that small flaws could serve as initiation sites for brittle fracture, if the flaws were subjected to yield loading below NDT temperature, and 2) that large scale crack arrest could be assumed at temperatures significantly above NDT, depending on nominal stress level.

Some engineers have misinterpreted the fracture analysis diagram to imply that structures should never be operated below NDT temperature, since small flaws are difficult to detect and yield point loads are always possible. In fact, most structures such as bridges, towers, rail, turbine rotors, etc., often experience service temperatures below NDT without failing or causing serious accidents. As indicated above, the low failure frequency results from the fact that

1) The probability that a large flaw exists in a region of high tensile stress is very low,

2) K_{Ic} is large at temperatures 50°C below NDT. Furthermore, there is little, if any, increase in K_{Ic} in going from say, NDT - 20°C to NDT + 20°C. Consequently, the probability of fracture initiation is already low, and it does not change dramatically at NDT (as may K_{ID}, Figure 9). Hence the relation of operating temperatures to NDT has little effect on fracture initiation, and

3) Structural reliability depends as much on the *scatter* in stresses, flaw size, and properties as it does on the absolute value of the parameters themselves.

The scatter in NDT temperatures, stress level, service temperatures actually makes the failure probability based on an NDT + x°C approach less reliable or optimal than some would believe, but still apparently conservative in view of the low number of brittle fractures that have occurred in structures operated well above NDT. The value in the approach is based primarily on its use for assuring crack arrest in those cases where the consequences of a brittle fracture are large.

Furthermore, the risk assessment should account for the fact that consequences of a brittle fracture are not necessarily high. Most structures show sufficient redundancy that even if a structural element fails by brittle fracture, the crack will be arrested by a bolted connection, or a second

element will take up the load, such that complete structural collapse does not occur, and many structural failures do not lead to serious personal injury or fatality, as few people are actually exposed.

In summary, the authors believe that combined risk analysis methods described above offer the most reasonable and efficient means to develop optimum selection of design stress, materials, structural configuration and inspection procedures to offer reasonable and inexpensive protection against brittle fracture and lead to minimum cost designs.

REFERENCES

1. STARR, C., "Benefit-Cost Studies in Socio-Technical Systems," Colloguim on Benefit-Risk Relationships for Decision-Making, Washington D.C., April 1971.
2. BESUNER, P.M., A. S. TETELMAN, G.R. EGAN and C.A. RAU, "The Combined Use of Engineering and Reliability Analysis in Risk Assessment of Mechanical and Structural Systems," Proceedings of Risk-Benefit Methodology and Application Conference, Asilomar, California, September 1975.
3. BENJAMIN, J.R. and CORNELL, C., Probability, Statistics and Decision Theory for Civil Engineers, McGraw-Hill, 1970.
4. JOHNSON, D.P., "Cost-Risk Optimization of Nondestructive Inspection Level," Failure Analysis Associates/Electric Power Research Institute Technical Report No. EPRI-217-1-5, September 1975 (submitted for Journal Publication).
5. PELLINI, W. and PUZAK, P., Naval Research Laboratory Report No. 5920, March 1963.

Table 1 Estimated Failure Rates for Bridges on Federal Aid Highways

No. of Bridges	Number Service Yrs.	Number of Failures	Failing Rate Per Bridge Year
64 Keywords - Steel, Steel Continuous, Suspension	2.473×10^3	1	4.04×10^{-4}
All U.S. Federal Highway National Bridge Inventory- 262,698 Bridges	$1.05 \times 10^{7*}$	10	9.5×10^{-7}
3 Bridges Known to Have Eyebars of 1060 Material	128	1	7.9×10^{-3}
14 Bridges Known to Have Eyebars of 1035 Material	550	0	0

*Based on average life of 40 years from 1st sample.

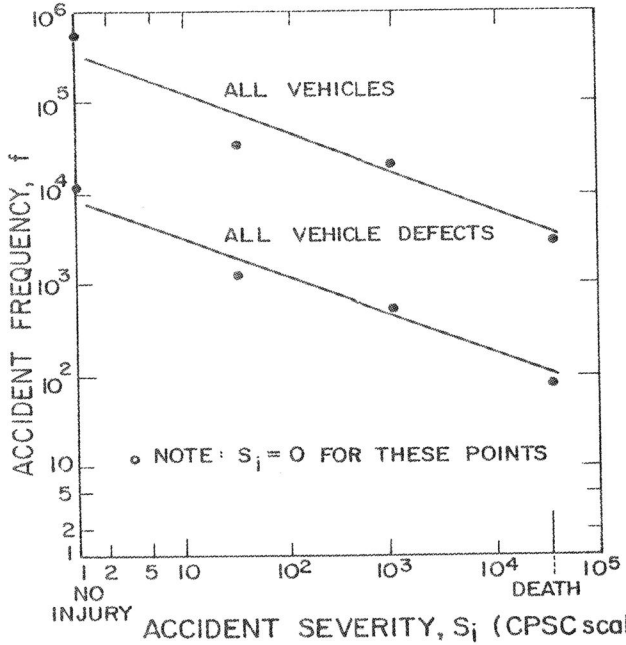

Figure 1 Automobile Accident Frequency - Severity Distribution (State of Texas 1971)

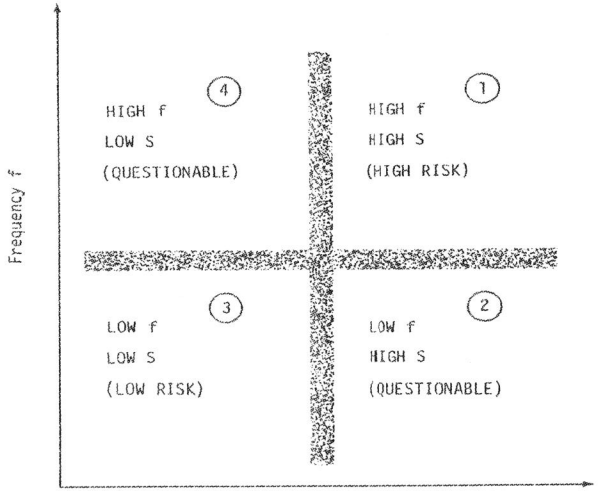

Figure 2 Breakdown of Frequency - Severity Plot into Four Areas

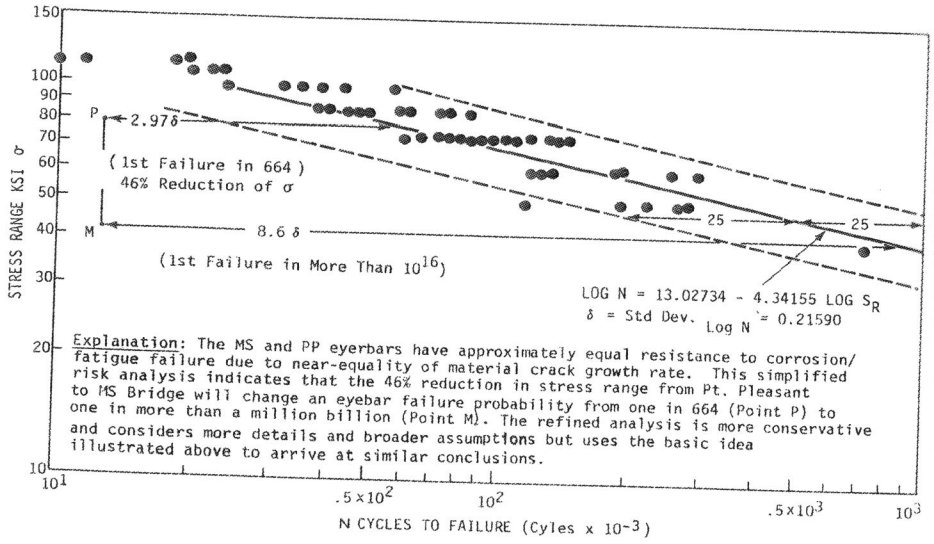

Figure 3 Simple Risk Analysis Using Fatigue Results of 1060 Eyebar Material with As-Received Surface

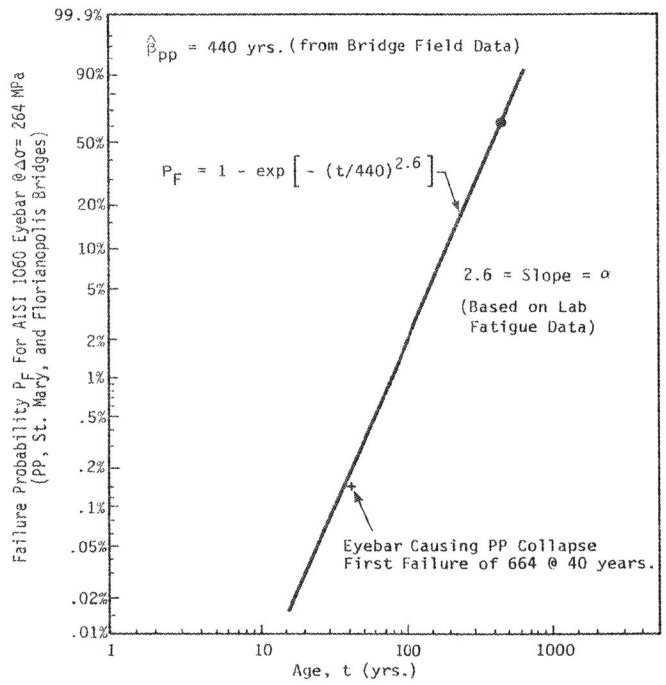

Figure 4 Estimated Failure Probability Distribution for Pt. Pleasant Type, AISI 1060 Eyebar. Characteristic Life β Estimated from Field Data Weibull Slope Scatter Parameter Estimated from Lab Data. Note Correlation Between First Failure and Estimated Distribution. ("PP" subscript denotes AISI 1060 eyebar).

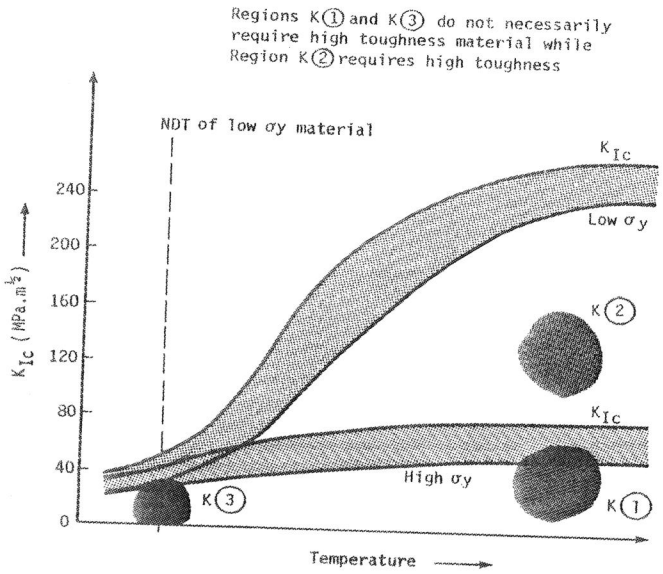

Figure 5 Schematic Comparison of Applied and Critical Stress Intensity Factor/Temperature Combinations for a Low and a High Toughness Material

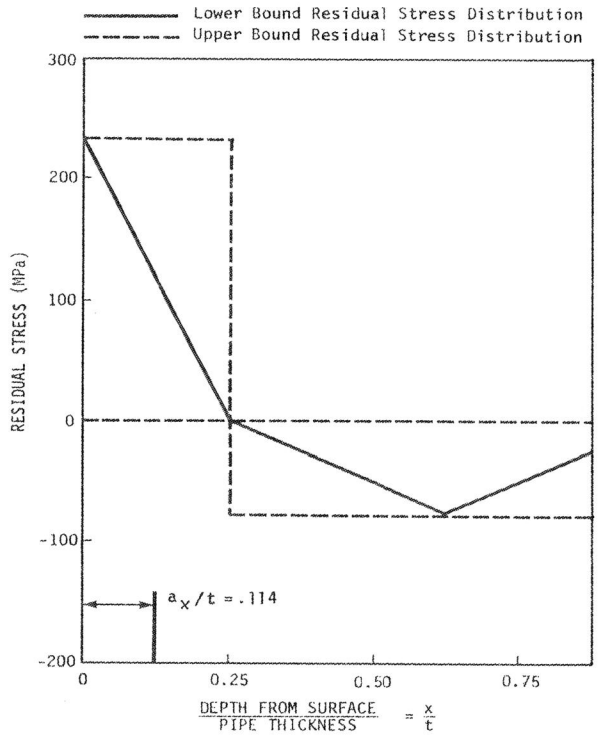

Figure 6 Assumed Distribution of Residual Stress Due to Gusset Weld for a Through Pipe Thickness.

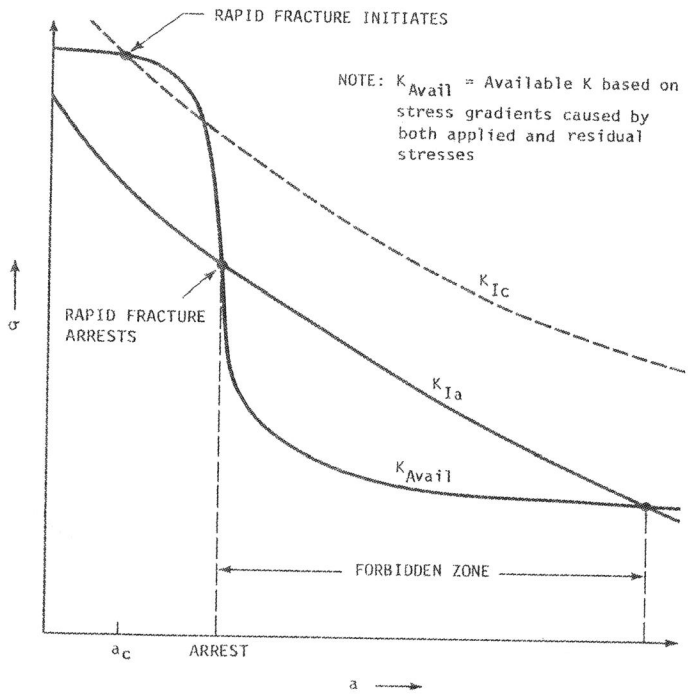

Figure 7 Schematic Representation of the Crack-Arresting Capability of a Material Subject to High Residual Stress which Initiates Rapid Brittle Fracture

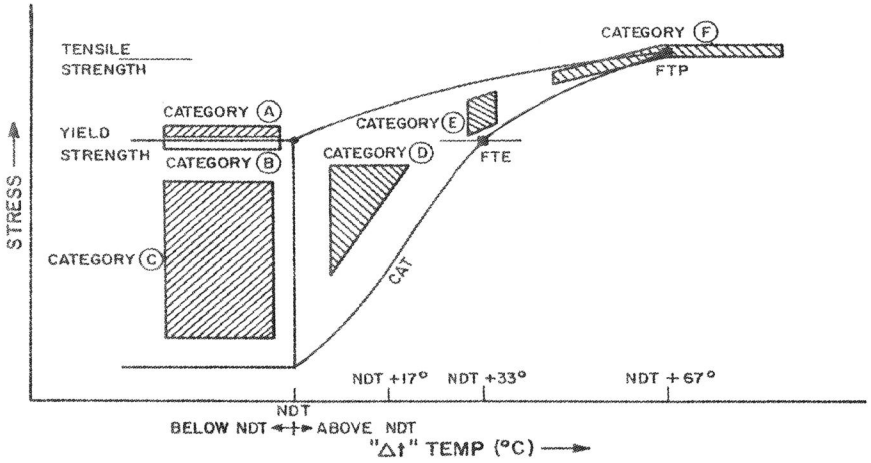

Figure 8 Sequence of the Discussion of Failure-Analysis Cases is Indicated by Categories A to F Referenced to Various Zones of the Fracture Analysis Diagram [after (5)]

Key to Figure 8

Category	Temperature	Flaw Size and Loading
A	Below NDT	Plastic strain loading of small flaws
B	Below NDT	High-level, residual stress loading of small flaws
C	Below NDT	Elastic stress loading of large flaws
D	Between NDT and CAT	Elastic stress loading of large flaws
E	At FTE	Plastic strain loading of moderately large flaws
F	Above FTE and FTP	Near ultimate tensile strength loading of very large flaws

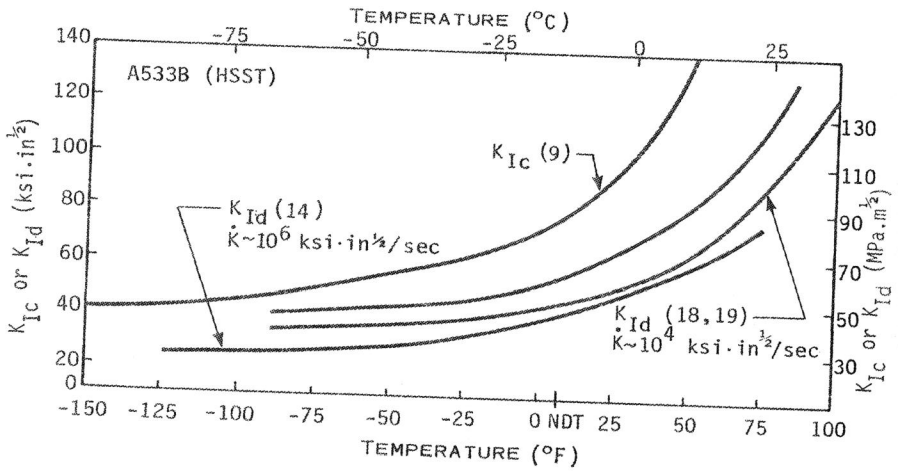

Figure 9 Comparison of Static, Dynamic and Instrumented Precracked Impact Fracture Toughness as a Function of Temperature for A 533 Steel [after (5)]